Simulation of Propagation of Coherent and Partially-Coherent Photon Beams Across Beamlines

O. Chubar, NSLS-II, BNL

"Round Beams" Mini-Workshop

SOLEIL, June 14 - 15, 2017

U.S. DEPARTMENT OF ENERGY

BROOKHAVEN NATIONAL LABORATORY

BROOKHAVEN SCIENCE ASSOCIATES

Outline

- SR Calculation Basics
- Wavefront Propagation Calculation using Fourier Optics and Compatible Methods
- Examples of Partially-Coherent SR Emission and Propagation Calculations for Beamlines in Low-Emittance Storage Rings
- Estimating Advantages of Round Beams by Simulations
- Conclusions

Emission by a Relativistic Charged Particle in Free Space: Retarded Potentials Approach

$$\mathbf{A} = e\int_{-\infty}^{+\infty} \boldsymbol{\beta}_e R^{-1}\delta(\tau - t + R/c)d\tau, \quad \varphi = e\int_{-\infty}^{+\infty} R^{-1}\delta(\tau - t + R/c)d\tau$$

(Gaussian CGS)

$$\Downarrow \quad \delta(t') = (1/2\pi)\int_{-\infty}^{+\infty}\exp(i\omega t')d\omega$$

$$\mathbf{A} = \frac{e}{2\pi}\int_{-\infty}^{+\infty}\exp(-i\omega t)d\omega\int_{-\infty}^{+\infty}\boldsymbol{\beta}_e R^{-1}\exp[i\omega(\tau + R/c)]d\tau$$

$$\varphi = \frac{e}{2\pi}\int_{-\infty}^{+\infty}\exp(-i\omega t)d\omega\int_{-\infty}^{+\infty}R^{-1}\exp[i\omega(\tau + R/c)]d\tau$$

Ternov used this approach to derive far-field SR expressions

$$\mathbf{E} = -\frac{1}{c}\frac{\partial \vec{A}}{\partial t} - \nabla\varphi = \frac{ie}{2\pi c}\int_{-\infty}^{+\infty}\omega\cdot\exp(-i\omega t)d\omega\int_{-\infty}^{+\infty}[\boldsymbol{\beta}_e - [1 + ic/(\omega R)]\cdot\mathbf{n}]R^{-1}\exp[i\omega(\tau + R/c)]d\tau$$

$$\Downarrow \quad \mathbf{E}_\omega \equiv \int_{-\infty}^{+\infty}\mathbf{E}\exp(i\omega t)dt$$

Exact expression, valid in the Near Field:

$$\mathbf{E}_\omega = iec^{-1}\omega\int_{-\infty}^{+\infty}[\boldsymbol{\beta}_e - [1 + ic/(\omega R)]\cdot\mathbf{n}]R^{-1}\exp[i\omega(\tau + R/c)]d\tau \qquad (\surd)$$

The equivalence of (√) to the well-known expression of Jackson can be shown by integration by parts

$$\mathbf{E}_\omega = ec^{-1}\int_{-\infty}^{+\infty}\frac{\mathbf{n}\times[(\mathbf{n} - \boldsymbol{\beta}_e)\times\boldsymbol{\beta}'_e] + cR^{-1}\gamma^{-2}(\mathbf{n} - \boldsymbol{\beta}_e)}{R\cdot(1 - \mathbf{n}\cdot\boldsymbol{\beta}_e)^2}\cdot\exp[i\omega(\tau + R/c)]d\tau$$

Emission by a Relativistic Charged Particle
Efficient Computation

Exact expression obtained from Retarded Potentials:

$$\mathbf{E}_{\omega} = iec^{-1}\omega \int_{-\infty}^{+\infty} [\boldsymbol{\beta}_e - [1 + ic/(\omega R)] \cdot \mathbf{n}] R^{-1} \exp[i\omega(\tau + R/c)] d\tau$$

Phase expansion valid in the Near Field:

$$\omega \cdot (\tau + R/c) \approx \Phi_0 + \frac{\pi}{\lambda} \left[s\gamma^{-2} + \int_0^s |\boldsymbol{\beta}_{e\perp}|^2 \, d\tilde{s} \quad + \quad \frac{(x - x_e)^2 + (y - y_e)^2}{z - s} \right]$$

Particle dynamics in external magnetic field:

$$\mathbf{r}_e = \mathbf{r}_e(s, \mathbf{r}_{e0}, \boldsymbol{\beta}_{e0}); \;\; \boldsymbol{\beta}_e \approx d\mathbf{r}_e / ds$$

Asymptotic expansion of the radiation integral (to accelerate computation):

$$\int_{-\infty}^{+\infty} F \exp(i\Phi) ds = \int_{s_1}^{s_2} F \exp(i\Phi) ds + \int_{-\infty}^{s_1} F \exp(i\Phi) ds + \int_{s_2}^{+\infty} F \exp(i\Phi) ds$$

$$\int_{-\infty}^{s_1} F \exp(i\Phi) ds + \int_{s_2}^{+\infty} F \exp(i\Phi) ds \approx \left[\left(\frac{F}{i\Phi'} + \frac{F'\Phi' - F\Phi''}{\Phi'^3} + \dots \right) \exp(i\Phi) \right]_{s_2}^{s_1}$$

Temporally-Incoherent and Coherent Spontaneous Emission by Many Electrons

Electron Dynamics:

$$\begin{pmatrix} x_e \\ y_e \\ z_e \\ \beta_{xe} \\ \beta_{ye} \\ \delta\gamma_e \end{pmatrix} = \mathbf{A}(\tau) \begin{pmatrix} x_{e0} \\ y_{e0} \\ z_{e0} \\ x'_{e0} \\ y'_{e0} \\ \delta\gamma_{e0} \end{pmatrix} + \mathbf{B}(\tau)$$

← Initial Conditions

Spectral **Photon Flux per unit Surface** emitted by the **whole Electron Beam:**

$$\frac{dN_{ph}}{dt dS (d\omega/\omega)} = \frac{c^2 \alpha I}{4\pi^2 e^3} \left\langle \left| \mathbf{E}_\omega \right|^2 \right\rangle$$

"Incoherent" SR

↓

$$\left\langle \left| \mathbf{E}_\omega \right|^2 \right\rangle = \int \left| \mathbf{E}_{\omega 0}(\mathbf{r}; x_{e0}, y_{e0}, z_{e0}, x'_{e0}, y'_{e0}, \delta\gamma_{e0}) \right|^2 f(x_{e0}, y_{e0}, z_{e0}, x'_{e0}, y'_{e0}, \delta\gamma_{e0}) dx_{e0} dy_{e0} dz_{e0} dx'_{e0} dy'_{e0} d\delta\gamma_{e0} +$$

$$+ (N_e - 1) \left| \int \mathbf{E}_{\omega 0}(\mathbf{r}; x_{e0}, y_{e0}, z_{e0}, x'_{e0}, y'_{e0}, \delta\gamma_{e0}) f(x_{e0}, y_{e0}, z_{e0}, x'_{e0}, y'_{e0}, \delta\gamma_{e0}) dx_{e0} dy_{e0} dz_{e0} dx'_{e0} dy'_{e0} d\delta\gamma_{e0} \right|^2$$

↑

Coherent SR

Common Approximation for CSR: **"Thin" Electron Beam:** $\left\langle \left| \mathbf{E}_\omega \right|^2 \right\rangle_{CSR} \approx N_e \left| \int_{-\infty}^{\infty} \tilde{f}(z_{e0}) \exp(ikz_{e0}) dz_{e0} \right|^2 \left| \mathbf{E}_{\omega 1} \right|^2$

For Gaussian Longitudinal Bunch Profile: $\left\langle \left| \mathbf{E}_\omega \right|^2 \right\rangle_{CSR} \approx N_e \exp(-k^2 \sigma_b^2) \left| \mathbf{E}_{\omega 1} \right|^2$

If $f(x_{e0}, y_{e0}, z_{e0}, x'_{e0}, y'_{e0}, \delta\gamma_{e0})$ is Gaussian, 6-fold integration over electron phase space can be done analytically for the (Mutual) Intensity of Incoherent SR and for the Electric Field of CSR

Wavefront Propagation in the Case of Full Transverse Coherence

Kirchhoff Integral Theorem applied to Spontaneous Emission by One Electron

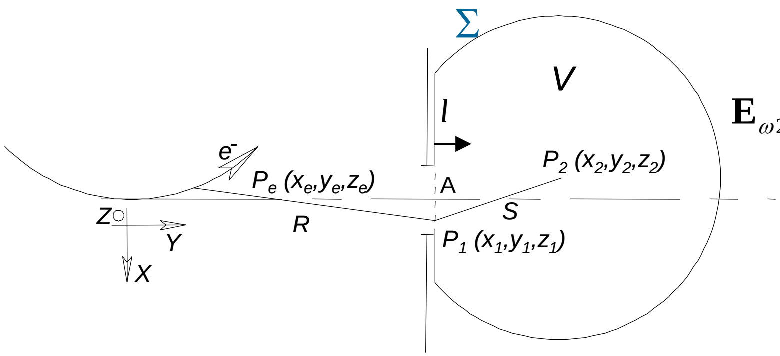

$$\mathbf{E}_{\omega 2\perp}(P_2) \approx \frac{k^2 e}{4\pi}\int_{-\infty}^{+\infty} d\tau \iint \frac{\boldsymbol{\beta}_{e\perp}-\mathbf{n}_{\perp}}{RS}\exp[ik(c\tau+R+S)]\cdot(\boldsymbol{l}\cdot\mathbf{n}_{p_e p_1}+\boldsymbol{l}\cdot\mathbf{n}_{p_1 p_2})d\Sigma$$

Valid at large observation angles;

Is applicable to complicated cases of diffraction inside vacuum chamber

Huygens-Fresnel Principle

$$\mathbf{E}_{\omega 2\perp}(P_2) \approx \frac{k}{4\pi i}\iint_A \mathbf{E}_{\omega 1\perp}(P_1)\frac{\exp(ikS)}{S}(\boldsymbol{l}\cdot\tilde{\mathbf{n}}+\boldsymbol{l}\cdot\mathbf{n}_{p_1 p_2})d\Sigma$$

Fourier Optics

Free Space:
(between parallel planes perpendicular to optical axis)

$$\mathbf{E}_{\omega 2\perp}(x_2,y_2) \approx \frac{k}{2\pi i L}\iint \mathbf{E}_{\omega 1\perp}(x_1,y_1)\exp[ik[L^2+(x_2-x_1)^2+(y_2-y_1)^2]^{1/2}]dx_1 dy_1$$

Assumption of small angles

“Thin” Optical Element:

$$\mathbf{E}_{\omega 2\perp}(x,y) \approx \mathbf{T}(x,y,\omega)\,\mathbf{E}_{\omega 1\perp}(x,y)$$

“Thick” Optical Element:
(propagation from transverse plane before the element to a transverse plane just after it)

$$\mathbf{E}_{\omega 2\perp}(x_2,y_2) \approx \mathbf{G}(x_2,y_2,\omega)\exp[ik\Lambda(x_2,y_2,k)]\,\mathbf{E}_{\omega 1\perp}(x_1(x_2,y_2),y_1(x_2,y_2))$$

"Economic" and Numerically Stable Version of the Free-Space Fourier-Optics Propagator

Huygens-Fresnel Principle:

(paraxial approximation)

$$\mathbf{E}_{\omega 2\perp}(x_2, y_2) \approx \frac{k}{2\pi i L} \iint \mathbf{E}_{\omega 1\perp}(x_1, y_1) \exp[ik[L^2 + (x_2 - x_1)^2 + (y_2 - y_1)^2]^{1/2}] dx_1 dy_1$$

Analytical Treatment of Quadratic Phase Term:

Before Propagation:

$$\mathbf{E}_{\omega 1\perp}(x_1, y_1) = \mathbf{F}_{\omega 1}(x_1, y_1) \exp\left[ik\frac{(x_1 - x_0)^2}{2R_x} + ik\frac{(y_1 - y_0)^2}{2R_y} \right]$$

After Propagation:

$$\mathbf{E}_{\omega 2\perp}(x_2, y_2) \approx \frac{k}{2\pi i L} \exp(ikL) \iint_{\Sigma} \mathbf{F}_{\omega 1}(x_1, y_1) \exp\left[ik\frac{(x_1 - x_0)^2}{2R_x} + ik\frac{(y_1 - y_0)^2}{2R_y} + ik\frac{(x_2 - x_1)^2 + (y_2 - y_1)^2}{2L} \right] dx_1 dy_1$$

$$= \frac{k}{2\pi i L} \exp\left[ikL + ik\frac{(x_2 - x_0)^2}{2(R_x + L)} + ik\frac{(y_2 - y_0)^2}{2(R_y + L)} \right] \times$$

$$\times \iint_{\Sigma} \mathbf{F}_{\omega 1}(x_1, y_1) \exp\left[ik\frac{R_x + L}{2R_x L}\left(x_1 - \frac{R_x x_2 + L x_0}{R_x + L} \right)^2 + ik\frac{R_y + L}{2R_y L}\left(y_1 - \frac{R_y y_2 + L y_0}{R_y + L} \right)^2 \right] dx_1 dy_1$$

$$= \mathbf{F}_{\omega 2}(x_2, y_2) \exp\left[ik\frac{(x_2 - x_0)^2}{2(R_x + L)} + ik\frac{(y_2 - y_0)^2}{2(R_y + L)} \right]$$

An Approach to High-Accuracy Partially-Coherent Emission and Wavefront Propagation Simulations

Averaging (over phase-space volume occupied by e-beam) of the intensity (or "mutual" intensity, or mathem. brightness) obtained from electric field emitted by an electron and propagated through an optical system:

$$I_{\omega}(x,y)=\int I_{\omega 1}(x,y;x_e,y_e,z_e,x'_e,y'_e,\delta\gamma_e)\ f(x_e,y_e,z_e,x'_e,y'_e,\delta\gamma_e)\,dx_e dy_e dz_e dx'_e dy'_e d\delta\gamma_e$$

$$I_{\omega 1}(x,y;x_e,y_e,z_e,x'_e,y'_e,\delta\gamma_e)=\left|\mathbf{E}_{\omega 1\perp}(x,y;x_e,y_e,z_e,x'_e,y'_e,\delta\gamma_e)\right|^2$$

$$M_{\omega 1}(x,y,\tilde{x},\tilde{y};x_e,y_e,z_e,x'_e,y'_e,\delta\gamma_e)=\mathbf{E}_{\omega 1\perp}(x,y;\ x_e,y_e,z_e,x'_e,y'_e,\delta\gamma_e)\mathbf{E}^{*}_{\omega 1\perp}(\tilde{x},\tilde{y};\ x_e,y_e,z_e,x'_e,y'_e,\delta\gamma_e)$$

$$B_{\omega 1}(x,y,\theta_x,\theta_y;x_e,y_e,z_e,x'_e,y'_e,\delta\gamma_e)\sim\mathbf{E}_{\omega 1\perp}(x,y;\ x_e,y_e,z_e,x'_e,y'_e,\delta\gamma_e)\int\mathbf{E}^{*}_{\omega 1\perp}(\tilde{x},\tilde{y};\ x_e,y_e,z_e,x'_e,y'_e,\delta\gamma_e)\exp\left[i\frac{\omega}{c}(\theta_x\tilde{x}+\theta_y\tilde{y})\right]d\tilde{x}d\tilde{y}$$

This method is general and accurate. For the most part, it is already implemented in SRW code. However, it can be CPU-intensive, requiring parallel calculations on a multi-core server or a small cluster. Several approaches are considered for increasing the efficiency, including use of low-discrepancy sequences (collaboration with R. Lindberg, K.-J. Kim, X. Shi, ANL), "improved Monte-Carlo" type techniques, as well as "coherent mode decomposition".

NOTE: the smaller the e-beam emittance (the higher the radiation coherence) – the faster is the convergence of simulations with this general method.

NOTE: convolution can be valid in some cases, such as pure projection geometry, focusing by a thin lens, diffraction at one slit, etc.

$$I_{\omega}(x,y)\approx\int\tilde{I}_{\omega 1}(x-\tilde{x}_e,y-\tilde{y}_e)\tilde{f}(\tilde{x}_e,\tilde{y}_e)\,d\tilde{x}_e d\tilde{y}_e$$

If convolution is valid, the calculations can be accelerated dramatically. The validity of the convolution relation can be easily verified numerically.

"Synchrotron Radiation Workshop" – Physical Optics Code for SR Emission and Propagation Calulations

First work on Wavefront Propagation applied to SR beamlines (PHASE code):
J. Bahrdt, Appl. Opt. 36 (19) 4367 (1997)

- First official version of SRW was developed at ESRF in 1997-98 (written in C++, interfaced to IGOR Pro); compiled versions are distributed from: http://www.esrf.eu/Accelerators/Groups/InsertionDevices/Software/SRW
- SRW was released to Open Source in 2012 under BSD type license.

The main Open Source repository, containing all C/C++ sources, C API, all interfaces and project development files, is on GitHub: https://github.com/ochubar/SRW

- SRW for Python (2.7.x and 3.x, 32- and 64-bit) cross-platform versions were released in 2012
- SRW development is partially supported by US DOE SBIR Program (BNL acts as subcontractor of RadiaSoft LLC, headed by D. Bruhwiler)
- SRW under Sirepo web interface is available since 2015: https://beta.sirepo.com/light#/home

Single-Electron (Fully Transversely-Coherent) UR Intensity Distributions, “in Far Field” and “at Source”

UR “Single-Electron” Intensity and “Multi-Electron” Flux

E-Beam Energy: 3 GeV
Current: 0.5 A
Undulator Period: 20 mm

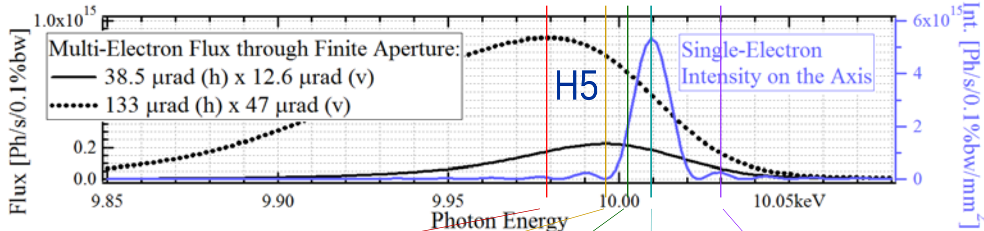

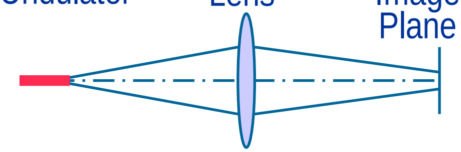

Intensity Distributions at 30 m from Undulator Center

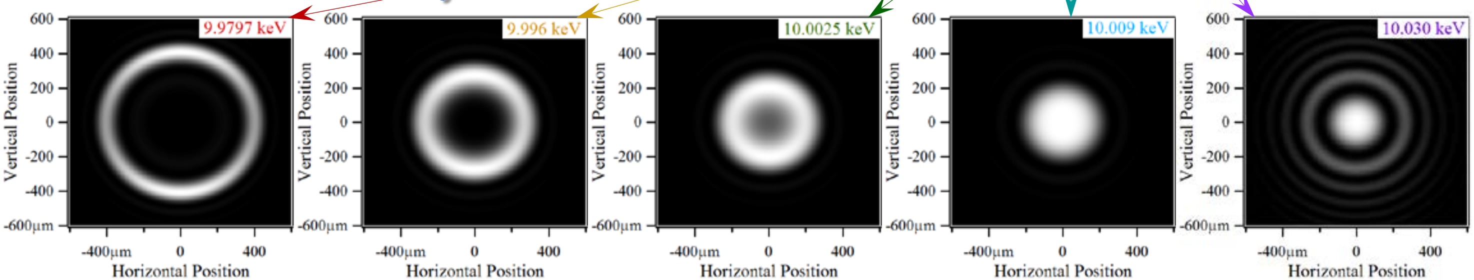

Vertical Cuts (x = 0)

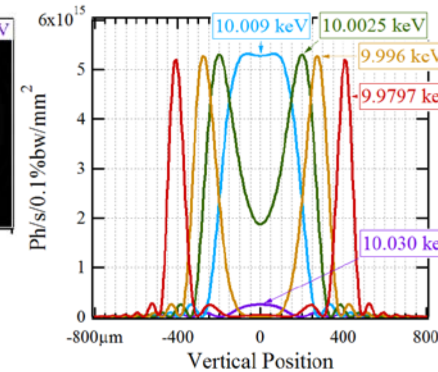

Intensity Distributions in 1:1 Image Plane

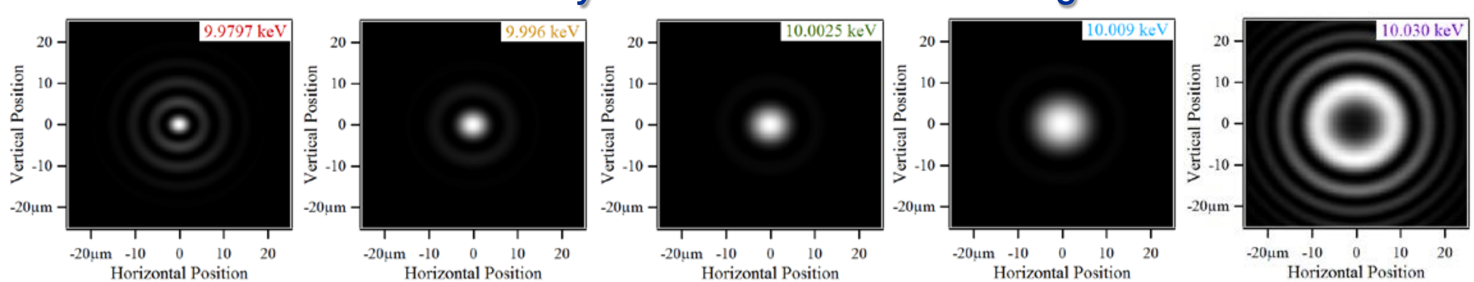

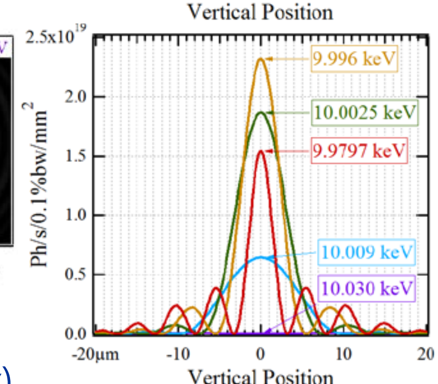

“Phase-Space Volume” Estimation for Vertical Plane

(RMS sizes/divergences calculated for the portions of intensity distributions containing 95% of flux)

$\sigma_y \sigma_y' \approx 7.7 \frac{\lambda}{4\pi}$ $\quad 3.3 \frac{\lambda}{4\pi}$ $\quad 1.9 \frac{\lambda}{4\pi}$ $\quad 1.5 \frac{\lambda}{4\pi}$ $\quad 9.2 \frac{\lambda}{4\pi}$

Calculated UR Intensity Distributions from Finite-Emittance Electron Beam, "in Far Field" and "at Source"

IVU20-3m Spectral Flux

through 100 µrad (H) x 50 µrad (V) Aperture
at K~1.5 providing H5 peak at ~10 keV

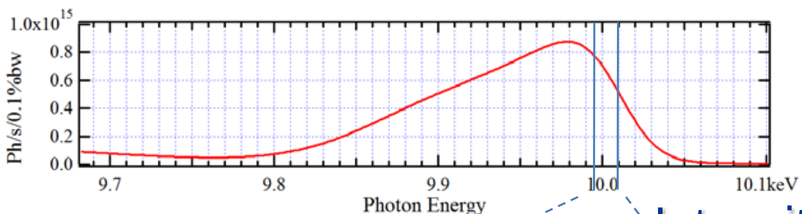

Electron Beam (NSLS-II):
- Hor. Emittance: 0.9 nm
- Vert. Emittance: 8 pm
- Energy Spread: 8.9×10^{-4}
- Current: 0.5 A
- Low-Beta Straight

Test Optical Scheme

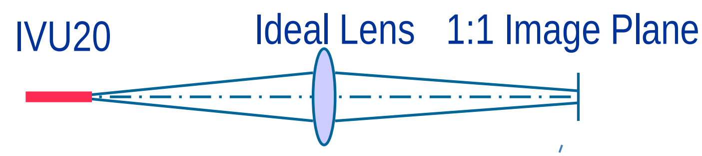

Intensity Distributions at ~10 keV

At 30 m from Undulator

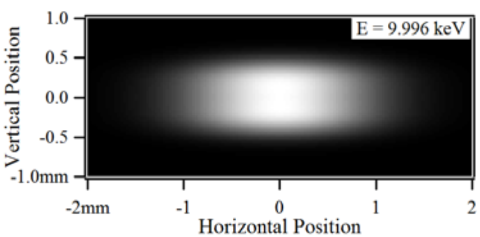

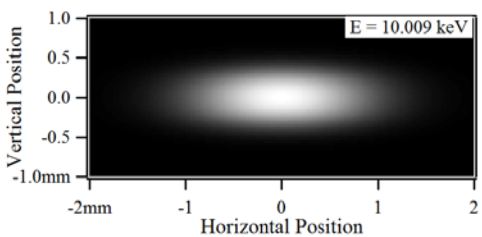

In 1:1 Image Plane

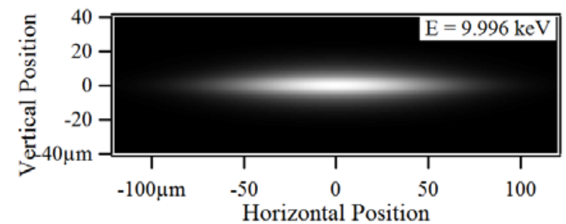

Horizontal Cuts (y = 0)

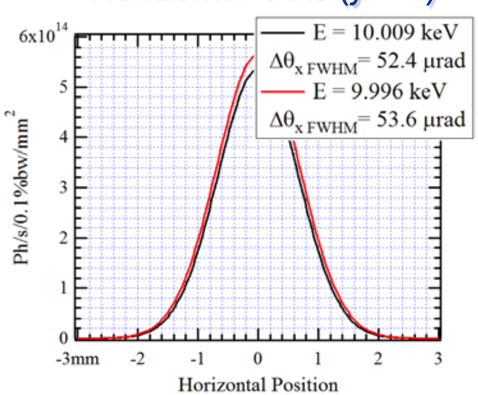

Vertical Cuts (x = 0)

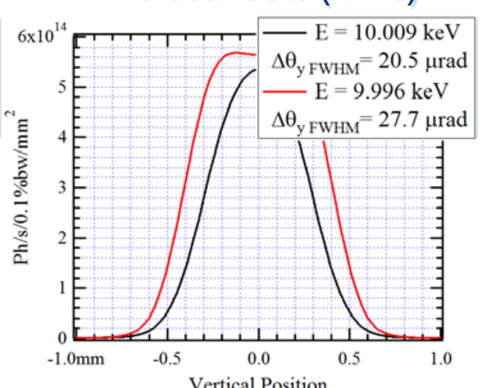

Horizontal Cuts (y = 0)

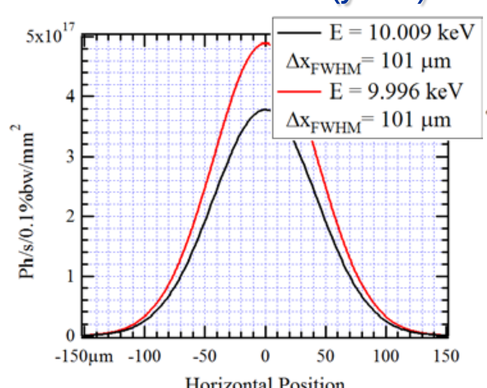

Vertical Cuts (x = 0)

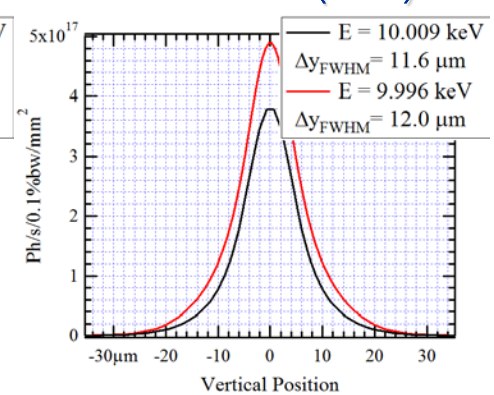

$\sigma_x \sigma_x' \approx \mathbf{97}\frac{\lambda}{4\pi}; \quad \sigma_y \sigma_y' \approx \mathbf{5.7}\frac{\lambda}{4\pi}$ …very far from Coherent Gaussian Beam !

NSLS-II Hard X-Ray Nanoprobe (HXN) Beamline Optical Layout and Wavefront Propagation Simulations

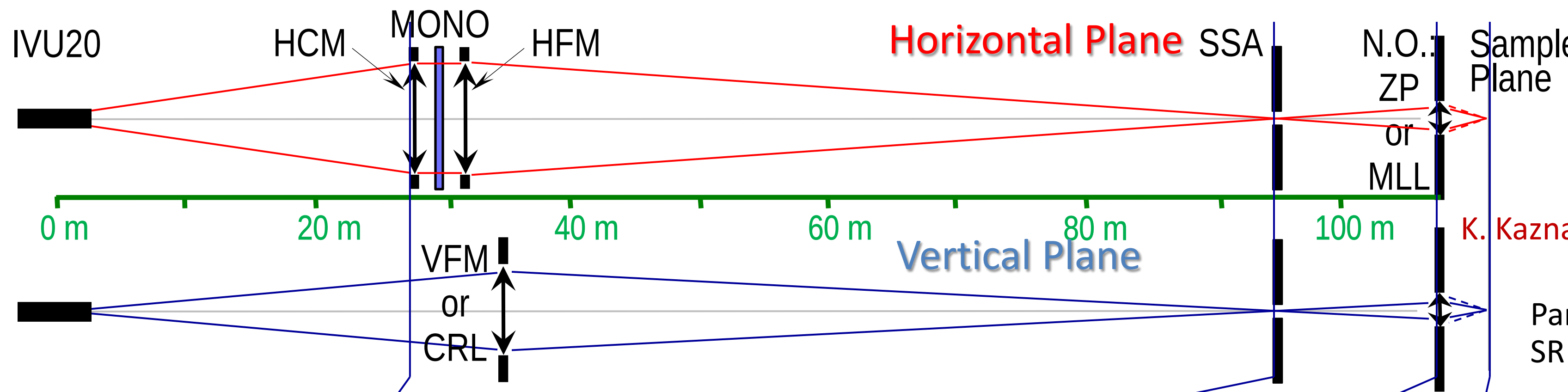

Y. Chu,
H. Yan,
K. Kaznatcheev

Pan-Am
SRI-2010

Flux after HCM: **~7.4x10^{14}** ph/s/.1%bw

Intensity Distributions

Flux within N.O. Aperture (d=150 μm): **~3.6 x10^{12}** ph/s/.1%bw

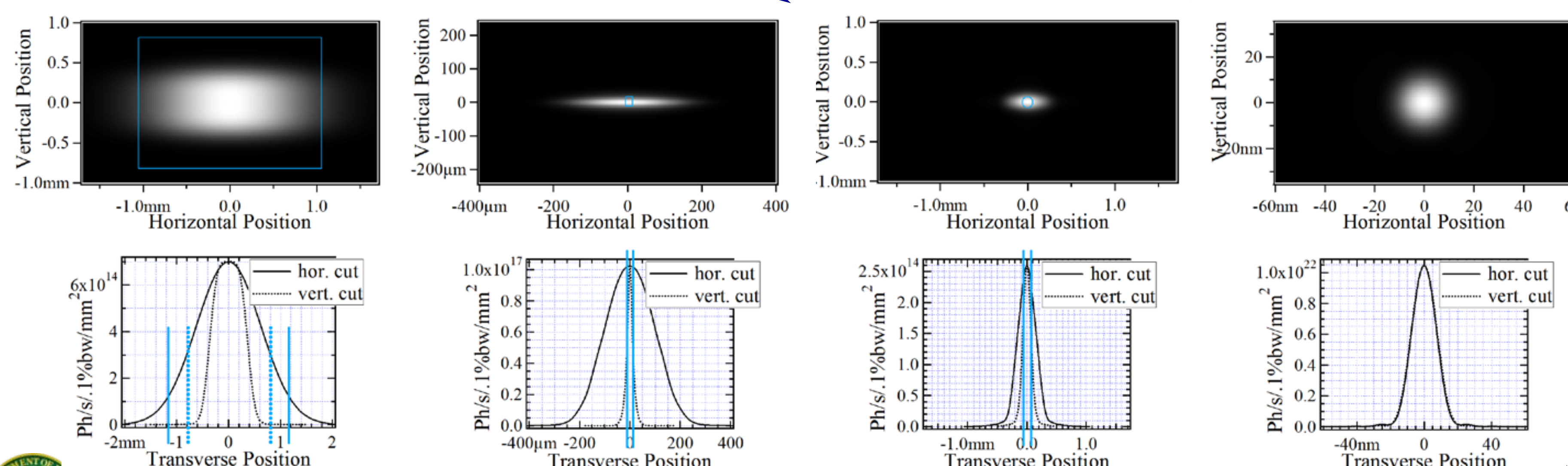

Intensity Distributions at Sample for Different Secondary Source Aperture Sizes at HXN (NSLS-II)

In Horizontal Median Plane (y = 0)

For Different Horizontal SSA Sizes (Δx_{ss})

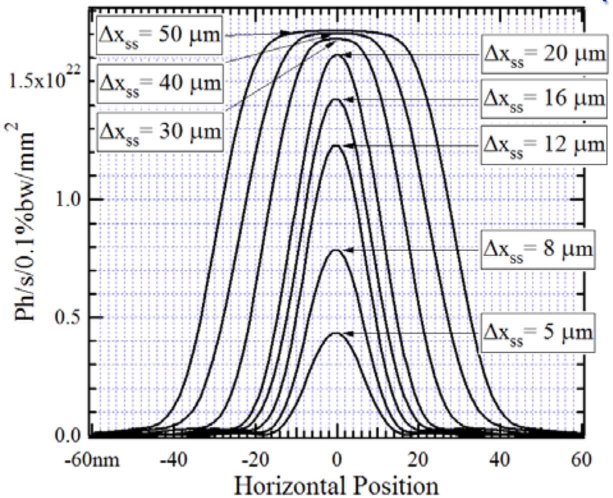

For Different Vertical SSA Sizes (Δy_{ss})

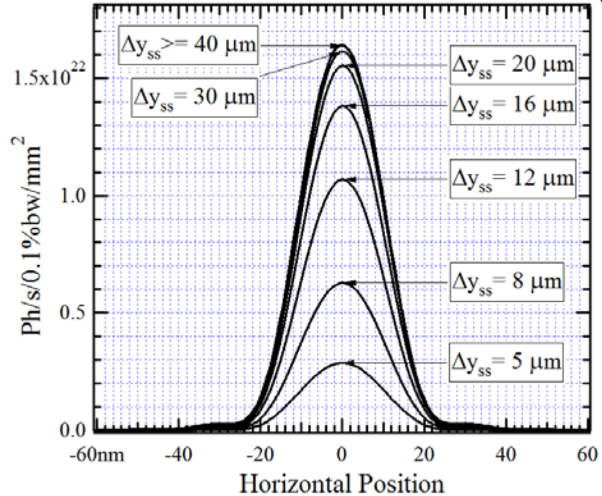

In Vertical Median Plane (x = 0)

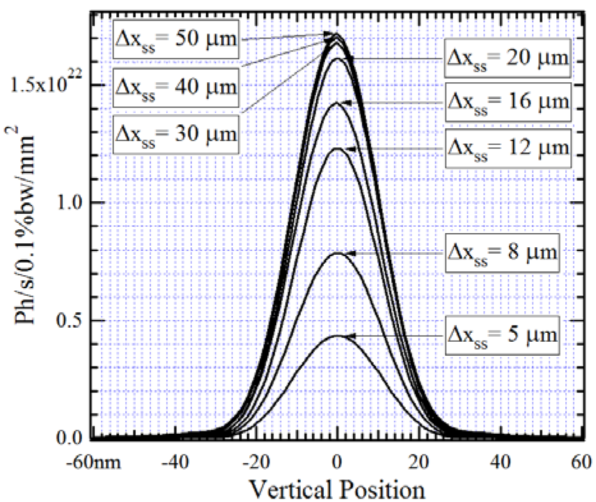

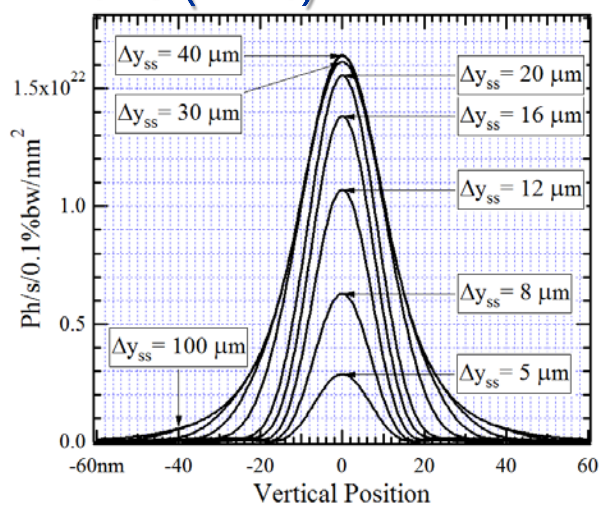

For Nanofocusing Optics with F = 18.14 mm, D = 150 μm ($\Delta r \approx$ 15 nm; $E_{ph} \approx$ 10 keV)
SSA located at 94 m, Nanofocusing Optics at 109 m from Undulator

Final Focal Spot Size and Flux vs Secondary Source Aperture Size (HXN, NSLS-II)

Horizontal Spot Size and Flux
vs Horizontal Secondary Source Aperture Size

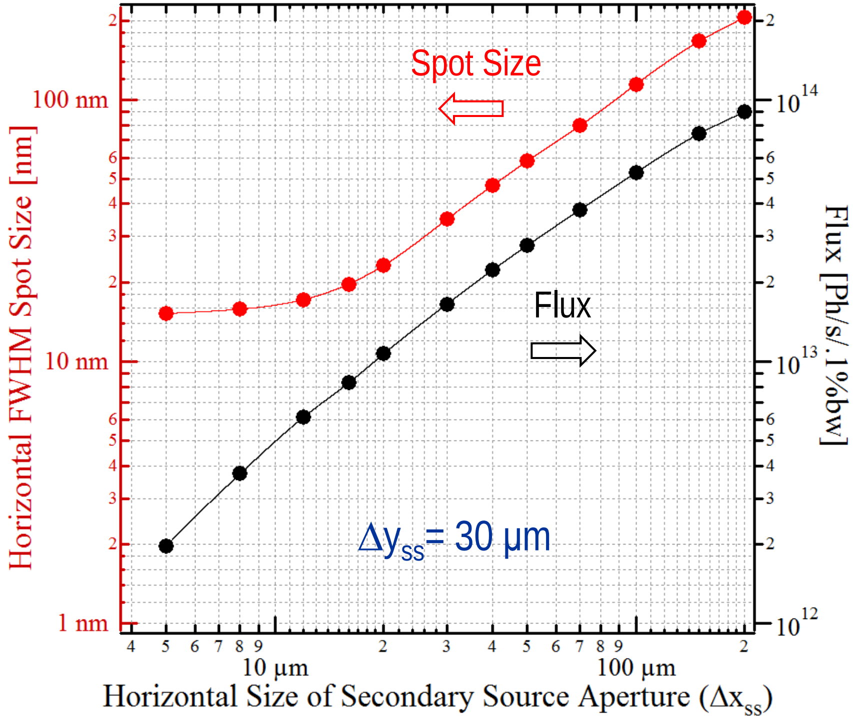

Vertical Spot Size and Flux
vs Vertical Secondary Source Aperture Size

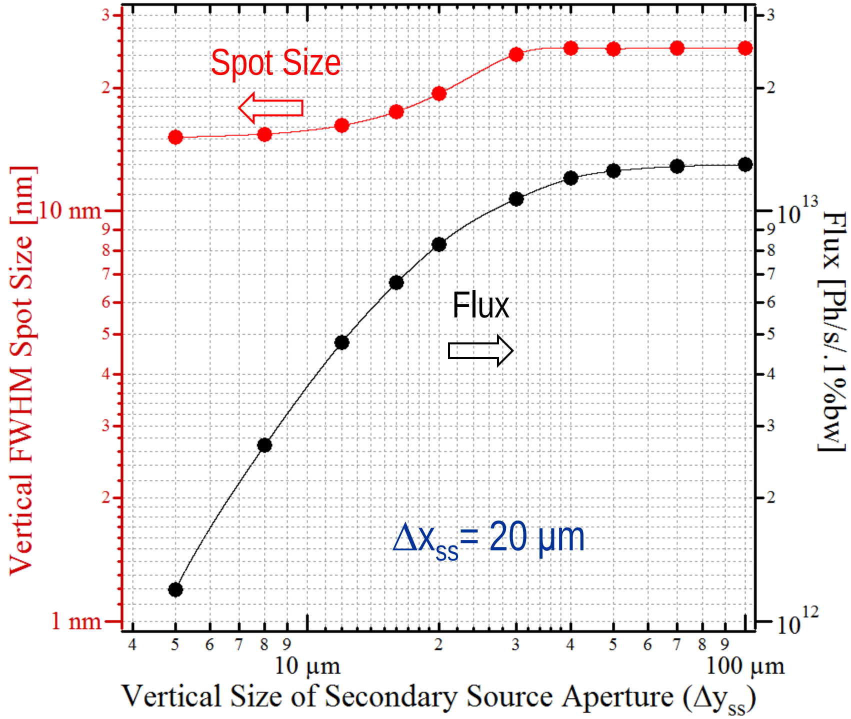

Secondary Source Aperture located at 94 m from Undulator
Spot Size and Flux calculated for Nanofocusing Optics simulated by Ideal Lens
with F = 18.14 mm, D = 150 μm located at 15 m from Secondary Source (109 m from Undulator)

NSLS-II Coherent Hard X-Ray (CHX) Beamline Optical Layout and Wavefront Propagation Simulations

A. Fluerasu
L. Wiegart

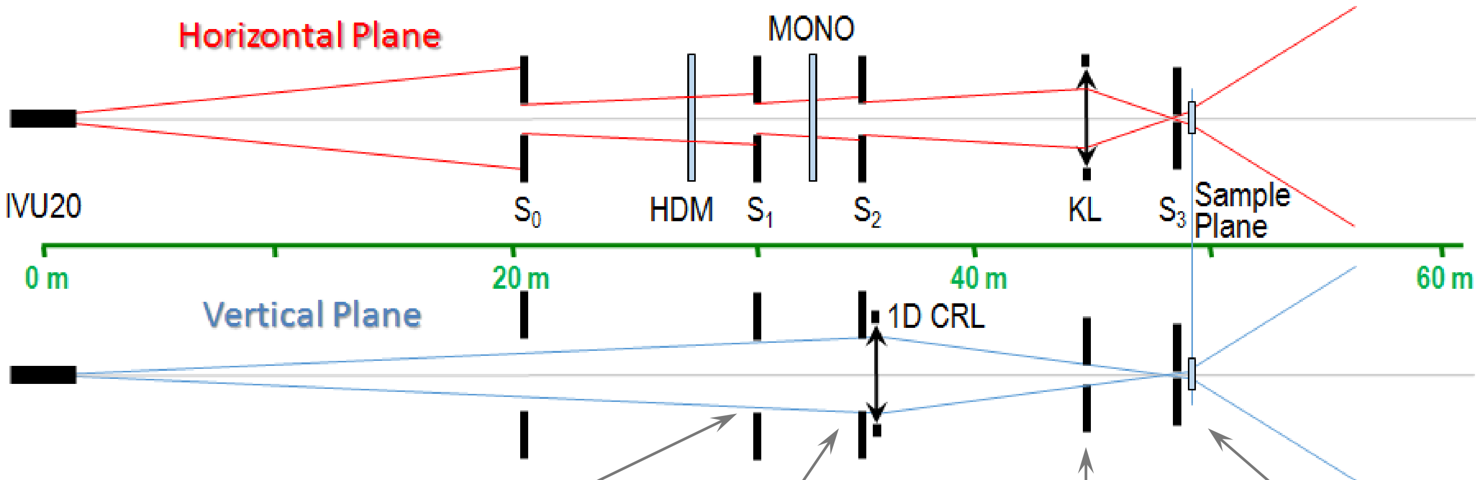

Intensity Distributions
for E = 10 keV
ΔS_{1x}= 44 μm
ΔS_{1y}= 1 mm

Before SS1 (@33.5 m)

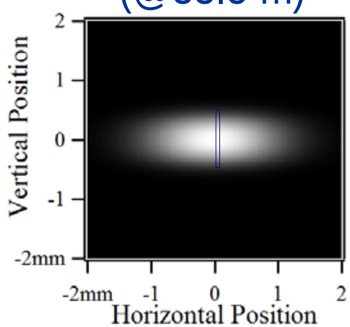

Before CRL (@35.8 m)

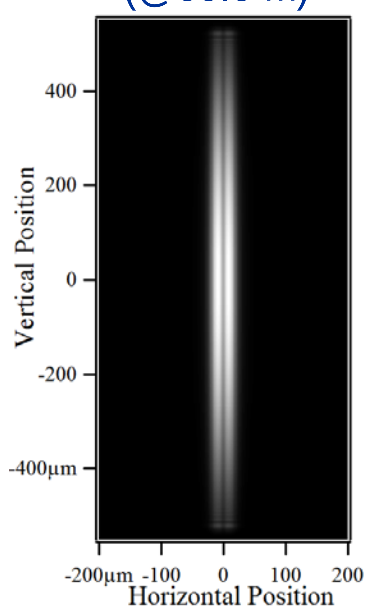

Before KL (@44 m)

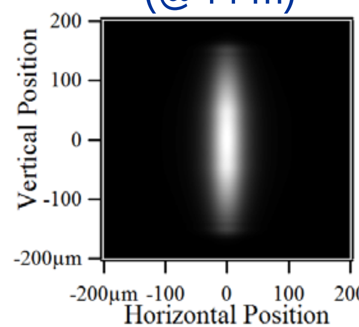

At Sample (@48.5 m)

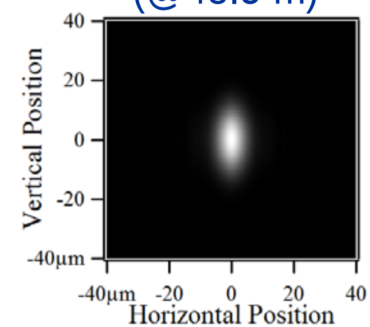

Flux: 10^{13} ph/s/.1%bw

Tracking Intensity and Degree of Transverse Coherence at Sample (CHX @ NSLS-II)

Intensity Distribution

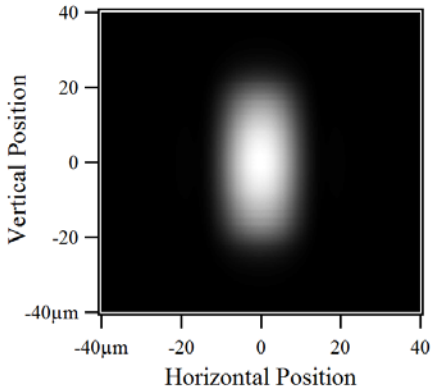

Degree of Transverse Coherence

In Horizontal Mid-Plane

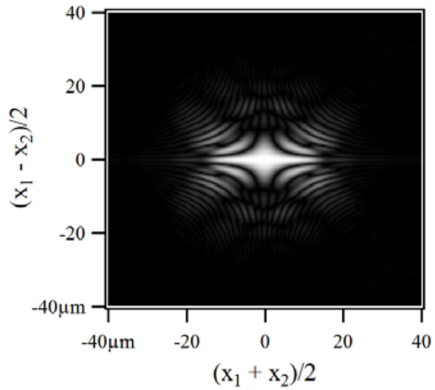

In Vertical Mid-Plane

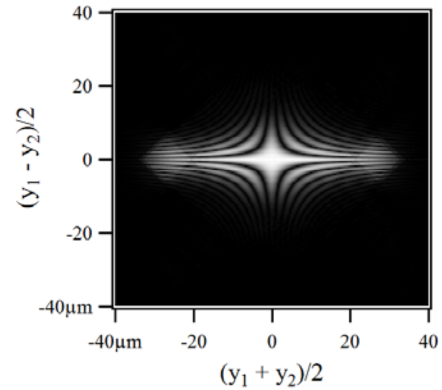

$$\mu(\boldsymbol{r}_1,\boldsymbol{r}_2,\omega) = |M(\boldsymbol{r}_1,\boldsymbol{r}_2,\omega)|/[M(\boldsymbol{r}_1,\boldsymbol{r}_1,\omega)M(\boldsymbol{r}_2,\boldsymbol{r}_2,\omega)]^{1/2}$$

$$M(\boldsymbol{r}_1,\boldsymbol{r}_2,\omega) \sim < \mathbf{E}_\perp(\boldsymbol{r}_1,\omega)\mathbf{E}_\perp^*(\boldsymbol{r}_2,\omega) >$$

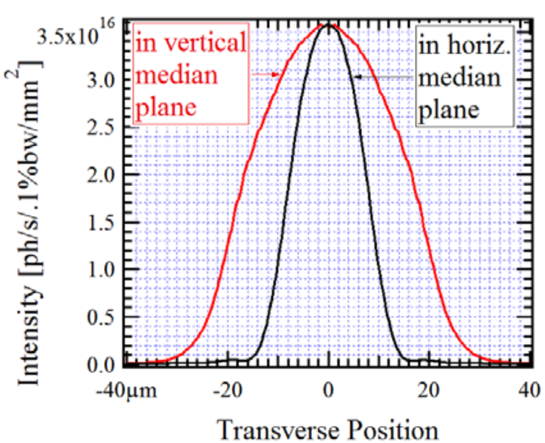

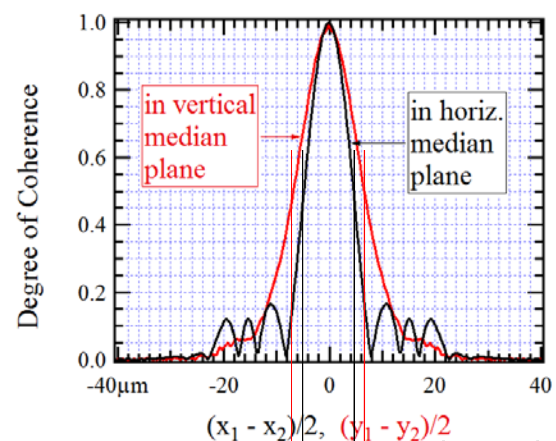

hor. coherence length: ~9.4 µm

vert. coherence length: ~13.4 µm

Angular Intensity (far field) after Two Slits separated by 10 µm

In Horizontal Plane (after vertical slits)

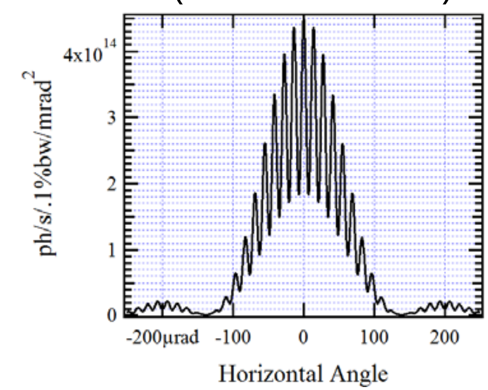

In Vertical Plane (after horizontal slits)

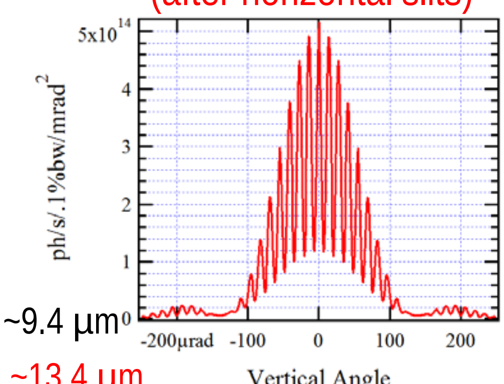

Good agreement with 2-slit interference simulation results

Towards Simulation of Complete Experiments (CHX @ NSLS-II)

Diffraction / Scattering from Test Sample

5000 “Silica Spheres”, d ≈ 200 nm

Partially-coherent simulations allow for identifying best conditions (/ beamline settings) for XPCS and many other types of experiments.

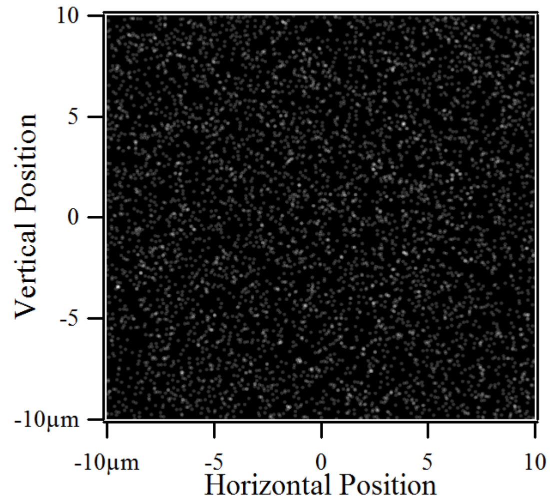

Sample simulation data from A.Fluerasu

Angular distribution of scattered X-rays at E=10 keV, ΔS_{1x}= 44 µm, ΔS_{1y}= 1 mm

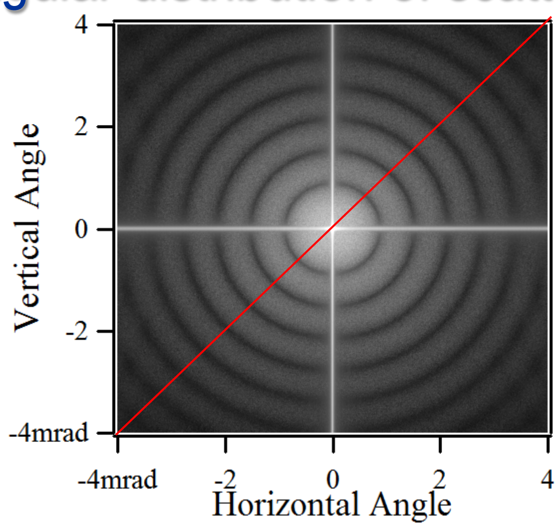

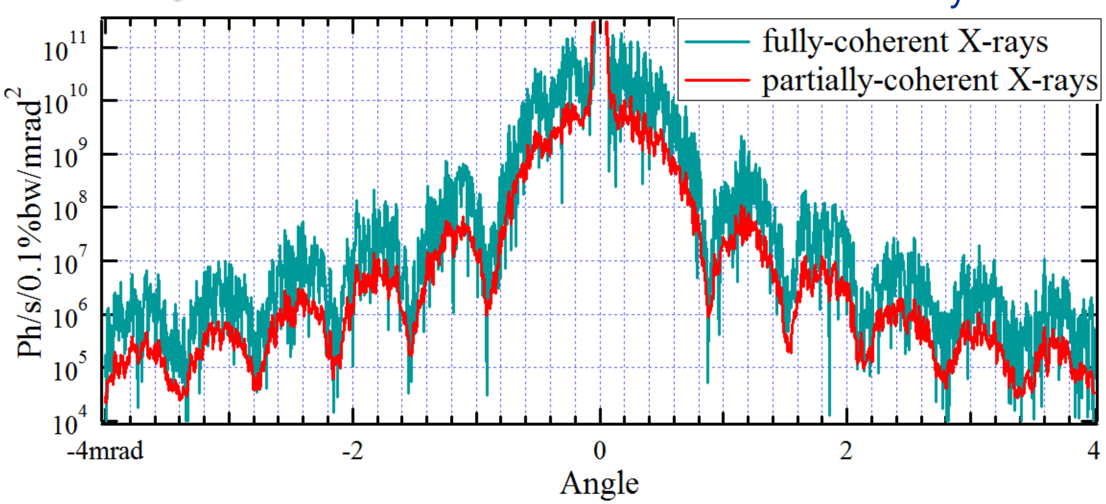

Attempting to Obtain Equal Horizontal and Vertical Spot Sizes and Coherence Lengths at CHX Sample (I)

Intensity Distributions

Degree of Transv. Coherence

Cuts vs Horizontal and Vertical Positions

Currently Attainable (at ε_x= 0.9 nm, β_x= 2 m, ε_y= 8 pm, β_y= 1 m)

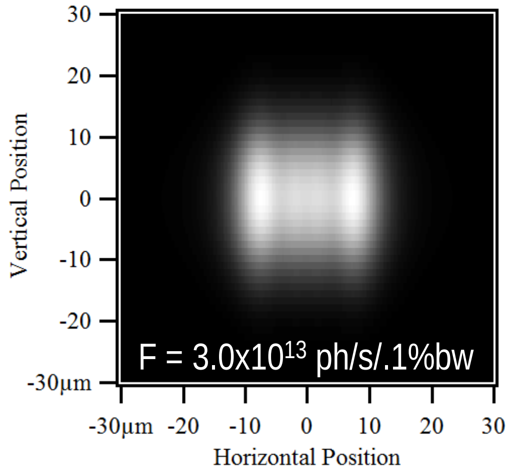

Spot Sizes: Δx = 22 µm, Δy = 20 µm

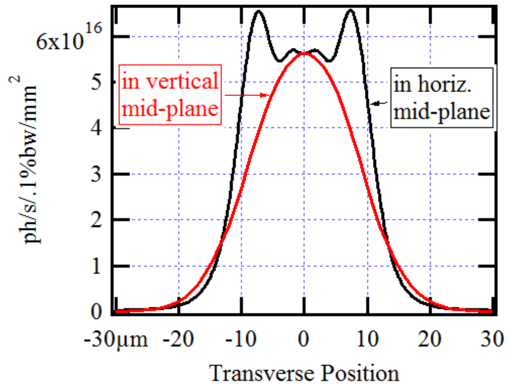

Coherence Lengths: l_x = 5.2 µm, l_y = 7.7 µm

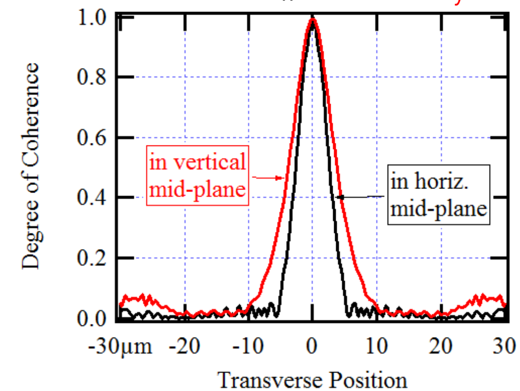

Would be Attainable with a "Round E-Beam" (at ε_x= ε_y= 85 pm, β_x= β_y= 2 m)

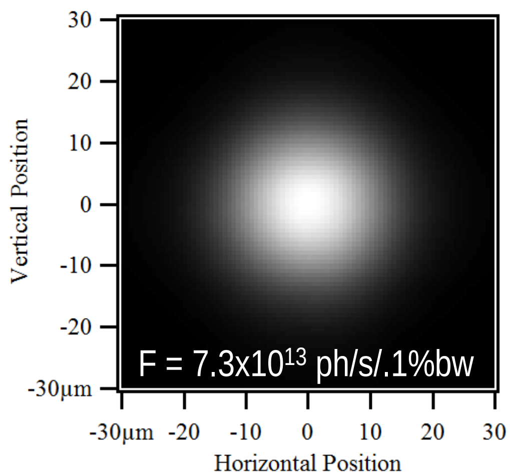

Spot Sizes: Δx = Δy = 22 µm

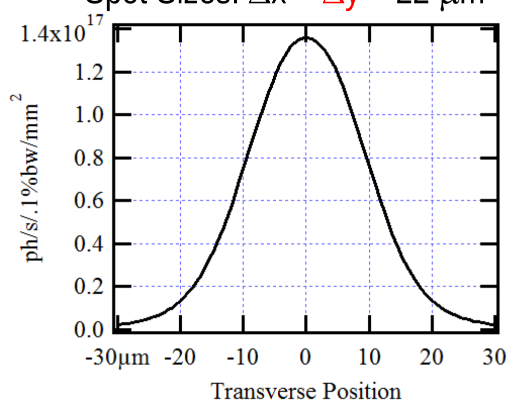

Coherence Lengths: l_x = l_y = 5.1 µm

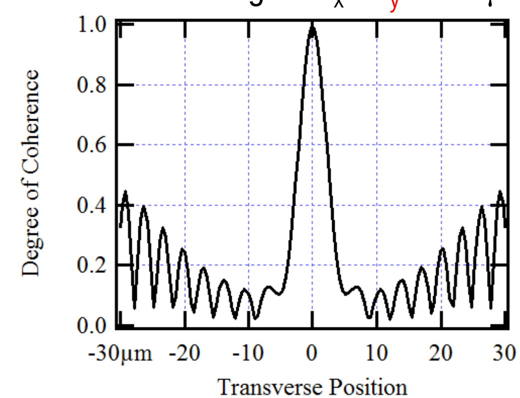

Attempting to Obtain Equal Horizontal and Vertical Spot Sizes and Coherence Lengths at CHX Sample (II)

Intensity Distributions | Degree of Transv. Coherence

Cuts vs Horizontal and Vertical Positions

Currently Attainable (at ε_x= 0.9 nm, β_x= 2 m, ε_y= 8 pm, β_y= 1 m)

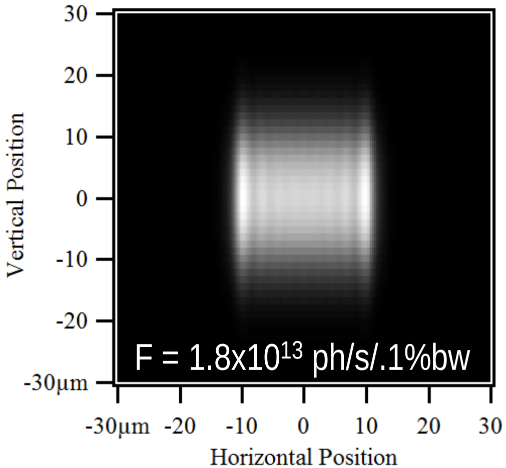

Spot Sizes: Δx = 22 µm, Δy = 20 µm

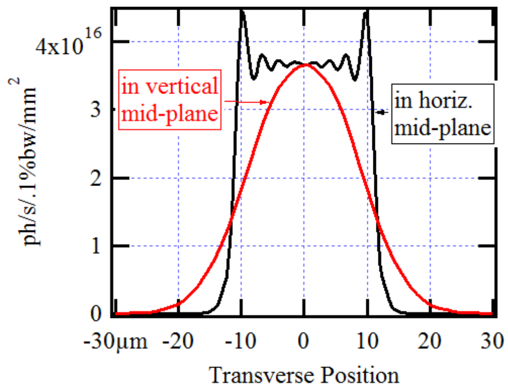

Coherence Lengths: l_x = 8.2 µm, l_y = 7.7 µm

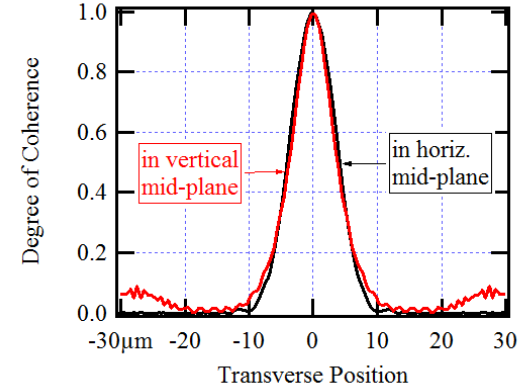

Would be Attainable with a "Round E-Beam" (at ε_x= ε_y= 85 pm, β_x= β_y= 2 m)

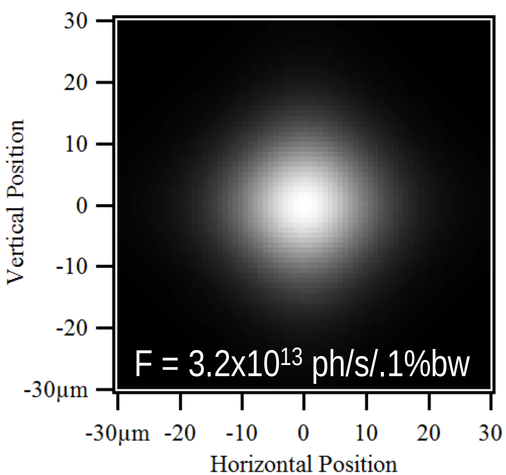

Spot Sizes: Δx = Δy = 19 µm

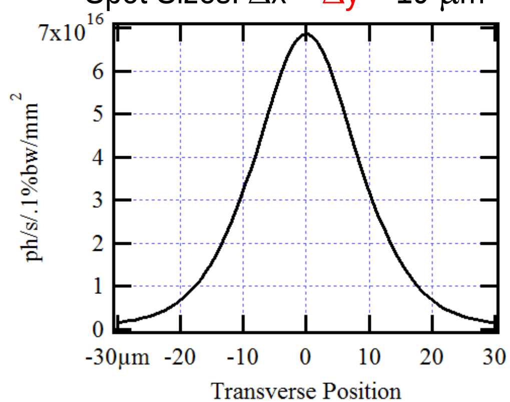

Coherence Lengths: l_x = l_y = 7.8 µm

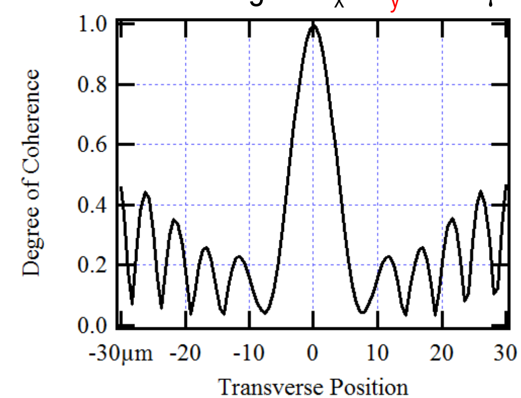

Conclusions

- High accuracy partially-coherent SR emission and propagation calculations for light sources are possible and (more-or-less) feasible with SRW code. Many applications are possible, including simulation of performances of IDs, X-ray optics in beamlines, and in some cases entire user experiments.
- Creating "round" electron beams in new low-emittance storage rings looks attractive for cases when round radiation spots at sample are required. This can result in gain in brightness and coherent flux and facilitates manipulations with / conditioning of X-ray beam. However, "matching" of single-electron UR angular divergences and source sizes with those of e-beam is important. Any particular case can be studied using partially-coherent simulations.

Acknowledgments

- Pascal Elleaume, Jean-Louis Laclare
- Colleagues who contributed to development of SRW:
  J. Sutter, D. Laundy (DLS),
  A. Suvorov, N. Canestrari, M. Rakitin (BNL),
  R. Reininger, X. Shi, R. Lindberg (ANL),
  L. Samoylova, A. Buzmakov (E-XFEL),
  D. Bruhwiler, R. Nagler (RadiaSoft LLC)
- SRW users:
  T. Shaftan, L. Wiegart, A. Fluerasu, K. Kaznatcheev, Y. Chu, M. Zhernenkov (BNL),
  J. Chavanne (ESRF),
  O. Marcouille, M.-E. Couprie, A. Ghaith (SOLEIL)
- Management and colleagues who helped in SRW transition to the Open Source:
  G. Materlik, K. Sawhney (DLS),
  J. Susini, M. S. del Rio (ESRF),
  S. Dierker, Q. Shen, P. Zschack, S. Hulbert (BNL),
  H. Sinn (E-XFEL)
- Many thanks to Pascale and Ryutaro – the Round Beam Workshop Organizers!